# Computationally efficient evaluation of fuel and electrical energy economy of plug-in hybrid electric vehicles with smooth driving constraints

# Computationally efficient evaluation of fuel and electrical energy economy of plug-in hybrid electric vehicles with smooth driving constraints

Pier Giuseppe Anselma,[a,b,*]

[a]*Department of Mechanical and Aerospace Engineering (DIMEAS), Politecnico di Torino, 10129 Torino, Italy*

[b]*Center for Automotive Research and Sustainable Mobility (CARS), Politecnico di Torino, 10129 Torino, Italy*

**Highlights**

- Optimal control of plug-in hybrid electric vehicle (HEV) powertrains.
- Smooth HEV driving constraints: thermal engine activations, gear shifts.
- Extension of a rapid near-optimal HEV control approach to plug-in HEVs.
- Benchmark with dynamic programming on real-world long-distance driving.

**Abstract**

Advanced computer-aided engineering tools are urgently needed to foster the development of electrified road vehicles that would enable abating fuel consumption and pollutant emissions of the transport sector. Concerning plug-in hybrid electric vehicles (HEVs), implementing an energy management strategy that can rapidly estimate near-optimal powertrain control trajectories while effectively dealing with broaded battery state-of-charge (SOC) window utilization and smooth HEV driving requirements still requires extensive development. To overcome the highlighted drawback, this paper introduces a formulation of the slope-weighted energy-based rapid control analysis (SERCA) algorithm which can rapidly identify near-optimal plug-in HEV control trajectories while complying with SOC boundaries and limiting the number of thermal engine activations and gear shifts. The HEV numerical model is introduced first, followed by formulating the optimal plug-in HEV control problem with smooth driving constraints and describing the dedicated SERCA based control approach. A performed case study demonstrates

* Corresponding author e-mail: pier.anselma@polito.it

that SERCA can identify smooth driving constrained near-optimal HEV control approaches for a 1.5 hour-long real-world driving mission within two minutes on a desktop computer, while a global optimal control approach such as dynamic programming (DP) is found to require more than 10 hours to perform the same task. On the other hand, compared with the global optimal reference provided by DP, the increase in estimated plug-in HEV operative cost in terms of fuel and electrical energy consumption associated to SERCA is always contained within few percentage points. The proposed methodology can accelerate HEV powertrain design and on-board supervisory controller development procedures.



Keywords: drivability, electrified powertrain, fuel economy evaluation, hybrid electric vehicle (HEV), optimal control, plug-in HEV, rapid control, real-world driving

## 1. Introduction

In recent years, transportation electrification has established as paradigm shift both in industry, academia, and society towards a sustainable transport system [1][2]. Indeed, several recent research studies have suggested how transportation electrification might lead to considerable environmental benefits in various geographical regions worldwide [3][4].

Accelerating the pace of transportation electrification advancement might be achieved through developing effective and computationally efficient computer-aided engineering tools [5]. Design and validation activities for the various sub-systems of electrified road vehicles might be rapidly and exhaustively performed in this way [6][7].

Plug-in hybrid electric vehicles (HEVs) have recently aroused as a viable technology to exploit medium range pure electric propulsion (e.g. for daily commuting), to improve the internal combustion engine (ICE) efficiency [8], to recover electrical energy while braking and to simultaneously avoid charge anxiety typically associated with pure electric vehicles [9]. Widespread adoption of plug-in HEVs could thus enable decarbonizing the transportation sector [10][11]. Nevertheless, additional complexity arises in a plug-in HEV when managing the power flow between ICE on one side and electric motor/generator (MG) on the other side which is linked to the high-voltage battery [12]. Indeed, the larger battery pack capacity compared to mild and full HEVs increases the priority and importance of activating the ICE in the right time instants within a given driving mission and of appropriately managing the power flow. Improperly splitting the propelling power between ICE and MG might indeed remarkably worsen the HEV performance even to the point where plug-in vehicle hybridization might be disadvantageous and no longer beneficial from fuel consumption and tailpipe emission points of view [13][14].

When evaluating the fuel and electrical energy economy capability of an HEV, off-line energy management strategies are generally implemented that assume knowing of the overall vehicle speed profile over time before performing the simulation [15]. Smooth HEV driving conditions should be ensured in this framework, including as example limiting the number of activations of the ICE and the number of gear shifts over time. Considering smooth driving conditions allows preserving vehicle drivability for the evaluated control solution (e.g. by avoiding gear hunting phenomena and noise-vibration-harshness issues entailed by frequent ICE de/activations). Among other possible advantages, this helps avoiding accelerated wear of the mechanical components of the drivetrain (e.g. clutches and shafts) [16].

Among off-line HEV energy management approaches, dynamic programming (DP) is a well-established algorithm capable of identifying the global optimal HEV control policy over an entire given driving mission [17][18]. Nevertheless, the main drawback of DP is notably associated with requiring a remarkable computational effort. This shortcoming becomes even more serious when considering plug-in HEVs due to the considerably higher number of discretized elements required for the state variable capturing the evolution of the high-voltage battery state-of-charge (SOC) over time [19]. Also, additional state variables are needed in DP to enable smooth HEV driving, which in turn further compromises the computational efficiency of the algorithm. In this

**Nomenclature**

*Acronyms*

| | |
|---|---|
| AMT | Automated manual transmission |
| DP | Dynamic programming |
| ECMS | Equivalent consumption minimization strategy |
| HEV | Hybrid electric vehicle |
| ICE | Internal combustion engine |
| MG | Motor/generator |
| PMP | Pontryagin's Minimum Principle |
| SERCA | Slope-weighted energy-based rapid control analysis |
| SOC | State-of-charge |
| WLTP | Worldwide harmonized light-vehicle test procedure |

*Symbols*

| | |
|---|---|
| $a$ | Vehicle acceleration |
| $Ah_{pack}$ | Battery pack capacity |
| $clutch_{state}$ | Clutch state |
| $c_{elec}$ | Electricity cost |
| $c_{fuel}$ | Fuel cost |
| $cost_{trip}$ | Total operative cost of the driving mission |
| $\Delta t$ | Simulaton time step |
| $E_{batt}$ | Net consumable battery energy |
| $F_{aero}$ | Vehicle aerodynamic drag |
| $F_{grad}$ | Grading resistance |
| $F_{misc}$ | Miscellaneous vehicle resistance |
| $F_{res}$ | Total vehicle resistive force |
| $F_{roll}$ | Vehicle rolling resistance |
| $\eta_{driveline}$ | Driveline efficiency |
| $\vartheta$ | Road slope |
| $g$ | Gravity acceleration |
| $I_{pack}$ | Battery pack current |
| $J_{DP}$ | DP cumulated cost function |
| $loss_{MG}$ | Electrical loss of MG |
| $M_{fuel}$ | Overall fuel consumption |
| $m_{veh}$ | Vehicle mass |
| $\dot{m}_{fuel}$ | Rate of fuel consumption |
| $\mu_{gear}$ | Penalization factor for gear shifting |
| $\mu_{ICE}$ | Penalization factor for ICE cranking |
| $n_{gear}$ | Gear number |
| $n_{gear,MAX}$ | Number of gears in the AMT |
| $N_{cranking,MAX}$ | Number of ICE activations allowed |
| $N_{shifts,MAX}$ | Number of gear shifts allowed |
| $OCV_{pack}$ | Open-circuit voltage of battery pack |
| $P_{aux}$ | Electrical power of auxiliaries |
| $P_{batt}$ | Battery power |
| $R_{pack}$ | Internal resistance of battery pack |
| $RL_A$ | Road load coefficient A |
| $RL_B$ | Road load coefficient B |
| $RL_C$ | Road load coefficient C |
| $\rho_{fuel}$ | Fuel density |
| $r_{wheel}$ | Wheel dynamic radius |
| $SOC$ | Battery SOC |
| $SOC_{end-SERCA}$ | Final battery SOC predicted by SERCA |
| $SOC_{min}$ | Minimum battery SOC |
| $SOC_{MAX}$ | Maximum battery SOC |
| $SOC_{target}$ | Target battery SOC |
| $\dot{SOC}$ | Battery SOC rate |
| $T_{ICE}$ | Torque of ICE |
| $T_{ICE\,min}$ | Minimum torque of ICE |
| $T_{ICE\,MAX}$ | Maximum torque of ICE |
| $T_{MG}$ | Torque of MG |
| $T_{MG\,min}$ | Minimum torque of MG |
| $T_{MG\,MAX}$ | Maximum torque of MG |
| $T_{wheels}$ | Torque at the wheels |
| $t$ | Current time instant |
| $t_{end}$ | Final time instant |
| $\tau_{diff}$ | Differential gear ratio |
| $\tau_{gear}$ | Transmission gear ratio |
| $v$ | Vehicle speed |
| $V_{OC}$ | Battery open-circuit voltage |
| $\omega_{ICE}$ | Rotational speed of ICE |
| $\omega_{ICE\,MAX}$ | Maximum rotational speed of ICE |
| $\omega_{idle}$ | Engine idle speed |
| $\omega_{MG}$ | Rotational speed of MG |
| $\omega_{MG\,MAX}$ | Maximum rotational speed of MG |

framework, the Pontryagin's Minimum Principle (PMP) is a solid alternative to DP as HEV control algorithm that can reduce the computational cost while identifying a near-optimal energy economy solution [20][21]. Nevertheless, each state variable in PMP involves considering a dedicated co-state parameter which needs tuning [22]. Each additional co-state parameter, introduced as example to reduce the number of ICE activations or gear shifts, exponentially increases the complexity of the overall calibration procedure for PMP, which mainly involves the shooting algorithm for tuning the values of co-state parameters [23]. Both the near optimality of the HEV control solution identified by PMP and the computational efficiency of the algorithm might be compromised in this way [24].

To overcome the drawbacks of both DP and PMP and to enable the rapid assessment of the HEV fuel and electrical energy economy capability while considering additional vehicle states, the author of this paper has recently introduced a heuristic near-optimal off-line HEV energy management approach named slope-weighted energy-based rapid control analysis (SERCA). The key idea behind the SERCA algorithm is to achieve the desired final value of battery SOC by means of an iterative procedure considering the net battery energy consumption of the HEV in the entire driving mission. Along with SERCA, few other HEV control approaches presented in the literature share this energy-based control approach which has been demonstrated computationally efficient. Related examples include the power weighted efficiency analysis for rapid sizing (PEARS) [25][26] and the efficiency evaluation real-time control strategy (EERCS) [27]. Compared with PEARS and EERCS, the enhanced flexibility, near-optimality and computational efficiency of the SERCA algorithm have been proved for various HEV powertrain architectures including parallel and series-parallel [28] and power-split [29]. Nevertheless, the effectiveness of SERCA has been demonstrated so far only when applied to HEV charge-sustaining operation, in which battery operation is controlled to limit the overall battery SOC variation throughout the driving mission. When simulating charge-depleting plug-in HEV operation, the energy management strategy needs to deal with broaden battery SOC window utilization. Appropriate care should therefore be taken in complying with the physical limitations for the battery SOC value over time, which is not covered in the current formulation of SERCA. This concern especially holds when simulating long-distance real-world driving missions (e.g. longer than 50 kilometres).

Compared with the HEV off-line control approaches reviewed from the literature, the main advantages of SERCA involve significantly enhancing computational efficiency while flexibly handling additional control constraints, for example in terms of smooth driving conditions [28]. However, the formulation of the SERCA algorithm currently considers HEV charge-sustaining operation only, i.e. without contribution of external battery electrical energy coming from the grid. To overcome the highlighted research gap, this paper introduces an improved formulation of the SERCA algorithm which allows simulating charge-depleting operation of plug-in HEVs. Among the key novelties brought by this paper, battery SOC physical limitations are accounted for when identifying the plug-in HEV control solution with SERCA for medium-distance and long-distance driving missions. Moreover, the introduced methodology ensures near optimality of the fuel economy and electrical energy economy of the plug-in HEV, remarkable computational efficiency and smooth HEV driving in terms of limited number of gear shifts and ICE activations. Rapidly assessing fuel and electrical energy economy capability as introduced by this paper is a fundamental milestone to enable: 1) the efficient and thorough exploration of the large design space for plug-in electrified powertrains to identify the best design and sizing candidates, 2) the rapid generation of off-line optimized control trajectories that allow training and benchmarking real-time capable plug-in HEV energy management systems. The rest of this paper is organized as follows: the parallel P2 plug-in HEV architecture is modelled first. The optimal plug-in HEV control problem with smooth driving constraints is then discussed, and DP is recalled as common approach to find the global optimal control solution. The following section aims at illustrating the extension of the SERCA algorithm to plug-in HEVs. A case study then involves simulating the plug-in HEV both in a standard drive cycle and in a long-distance driving mission to demonstrate the effectiveness of SERCA by

benchmarking with DP in terms of fuel and electrical energy economy capability and computational efficiency. Conclusions are finally drawn.

## 2. Plug-in HEV model

The numerical model implemented in this work for simulating a plug-in HEV finds discussion in this section. A parallel P2 hybrid electric powertrain architecture has been selected which finds illustration in Fig. 1. This choice stems from efficiency and technological potential for the parallel P2 HEV layout [30]. Moreover, the current formulation of SERCA for parallel HEVs in charge-sustaining operation was demonstrated for a P2 powertrain architecture as well [28]. In a P2 HEV powertrain, torques of the ICE and of the MG are additive, and their respective contributions are summed upstream the automated manual transmission (AMT) [31]. For this reason, P2 electrified powertrains are also known as pre-transmission parallel HEVs. In the follow-up of this section, fundamentals for modeling the HEV propulsion sub-systems according to the commonly adopted backward quasi-static approach will be recalled [32].

### *2.1. Vehicle body and road load*

The total vehicle resistive force $F_{res}$ can be easily computed from the vehicle free body diagram using (1):

$$F_{res} = F_{aero} + F_{roll} + F_{misc} + F_{grad} \quad (1)$$

where $F_{aero}$ is the aerodynamic drag, $F_{roll}$ stands for the rolling resistance, $F_{misc}$ incorporates some miscellaneous terms whereas $F_{grad}$ is the grading resistance related to road slope angle $\vartheta$. Specifically, the aforesaid resistive terms have been evaluated as follows:

$$F_{aero} + F_{roll} + F_{misc} = RL_A \cdot sign(v) + RL_B \cdot v + RL_C \cdot v^2 \quad (2)$$

$$F_{grad} = m_{veh} \cdot g \cdot sin\vartheta \quad (3)$$

where $RL_A$, $RL_B$ and $RL_C$ are the vehicle road load coefficients, $v$ is the longitudinal speed of the vehicle, $g$ stands for the gravitational acceleration, and $m_{veh}$ is the total mass of the vehicle in kilograms. Then, the torque requested at the wheels $T_{wheels}$ to either propel or brake the vehicle can be computed according to (4):

$$T_{wheels} = (F_{res} + m_{veh} \cdot a) \cdot r_{wheel} \quad (4)$$

where $a$ indicates the longitudinal acceleration of the vehicle, while $r_{wheel}$ is the wheel dynamic radius.

### *2.2. Driveline*

Moving to the HEV driveline, the torque balance equation at the input shaft of the AMT can be written as:

$$T_{ICE} \cdot clutch_{state} + T_{MG} = \frac{T_{wheels}}{\tau_{diff} \cdot \tau_{gear}(n_{gear}) \cdot \eta_{driveline}^{sign(T_{wheels})}} \quad (5)$$

where $T_{ICE}$ and $T_{MG}$ are the torques of the ICE and the MG, respectively. $\tau_{diff}$ and $\tau_{gear}(n_{gear})$ stand for the differential gear ratio and the gear ratio related to the given gear number engaged $n_{gear}$. $\eta_{driveline}$ is the driveline efficiency, which is powered by the sign of $T_{wheels}$ to account for both propelling and braking events. Finally, $clutch_{state}$ is a binary variable which is equal to 0 or 1 when the clutch in Fig. 1 is disengaged or engaged, respectively.

As far the speeds of power components are concerned, these can be calculated as follows:

$$\omega_{MG} = \frac{v \cdot \tau_{diff} \cdot \tau_{gear}(n_{gear})}{r_{wheel}} \quad (6)$$

$$\omega_{ICE} = \omega_{MG} \cdot clutch_{state} \quad (7)$$

Where $\omega_{MG}$ and $\omega_{ICE}$ are the rotational speeds of MG and ICE, respectively.

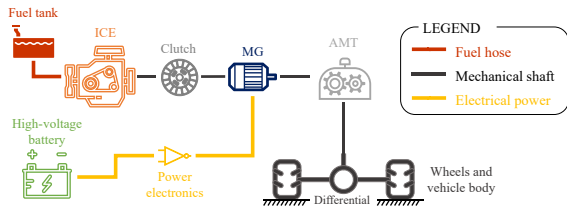


Fig. 1. Schematic diagram of the HEV powertrain architecture considered in this work.

### 2.3. High-voltage battery

When it comes to the high-voltage battery, the electrical power $P_{batt}$ that it is required to either deliver or absorb can be expressed as:

$$P_{batt} = \omega_{MG} \cdot T_{MG} + loss_{MG}(\omega_{MG}, T_{MG}) + P_{aux} \quad (8)$$

Where $loss_{MG}$ is the electrical power loss of the MG which can be evaluated at each time instant by interpolating in a two-dimensional lookup table with speed and torque of the MG as independent variables. Finally, $P_{aux}$ stands for the electrical power of the auxiliaries (e.g. lubrication, lighting) and it is assumed here being constant over time.

Then, the current of the high-voltage battery pack $I_{pack}$ can be evaluated by considering an equivalent circuit approach as expressed in (9).

$$I_{pack} = \frac{OCV_{pack}(SOC) - \sqrt{OCV_{pack}^2(SOC) - 4 \cdot P_{batt} \cdot R_{pack}(SOC)}}{2 \cdot R_{pack}(SOC)} \quad (9)$$

$OCV_{pack}$ and $R_{pack}$ are the open-circuit voltage and the internal resistance of the high-voltage battery pack, which are interpolated in a one-dimensional lookup table with SOC as independent variable.

Finally, the SOC of the high-voltage battery pack can be evaluated by considering the vector of the discrete $t_{end}$ time instants for the retained driving mission using (10):

$$SOC(t_{end}) = SOC(0) - \sum_{t=1}^{t_{end}} \dot{SOC}(t) \cdot \Delta t = SOC(0) - \sum_{t=1}^{t_{end}} \frac{I_{pack}(t)}{Ah_{pack} \cdot 3600} \cdot \Delta t \quad (10)$$

where $t_{end}$ stands for the final time instant of the driving mission as well. $\dot{SOC}$ is the instantaneous variation of battery SOC. $SOC(0)$ and $Ah_{pack}$ stands for the battery SOC at the beginning of the driving mission and the capacity of the high-voltage battery pack in ampere-hours, respectively. $\Delta t$ is the simulation time step, which is set to 1 second here.

### 2.4. ICE

The ICE fuel consumption $M_{fuel}$ in the overall driving mission under analysis can be written as:

$$M_{fuel} = \sum_{t=1}^{t_{end}} \dot{m}_{fuel}[\omega_{ICE}(t), T_{ICE}(t), clutch_{state}(t)\,] \cdot \Delta t \quad (11)$$

where $\dot{m}_{fuel}$ is the instantaneous fuel consumption rate in grams/second which can be evaluated by interpolating in a steady-state two-dimensional lookup table as function of ICE rotational speed and torque request. It should be noted that $\dot{m}_{fuel}$ is set to 0 in those time instants in which $clutch_{state}$ is equal to 0, denoting ICE at rest.

## 3. Optimal plug-in HEV control with smooth driving constrains

In this section, the optimal control of the parallel P2 plug-in HEV powertrain architecture finds discussion. The retained formulation of the optimal HEV control problem with smooth driving constraint is detailed first. Then, DP is recalled as a common approach to find the global optimal solution for the introduced control problem.

### 3.1. Optimal HEV control problem

The retained formulation of the optimal control problem considering a parallel P2 plug-in HEV powertrain layout and smooth driving constraints can be expressed as in (12).

$$\arg\min \left\{ cost_{trip} = \sum_{t=1}^{t_{end}} \left[ c_{fuel} \cdot \frac{\dot{m}_{fuel}(t)}{\rho_{fuel}} \cdot \Delta t + c_{elec} \cdot \left( \frac{OCV_{pack}(t) \cdot I_{pack}(t) \cdot \Delta t}{3.6e6} \right) \right] \right\}$$

subject to:

Mechanical constraints:

$$\begin{gathered} 1 \le n_{gear}(t) \le n_{gear,MAX} \\ \omega_{idle} \le \omega_{ICE}[t, clutch_{state}(t) = 1\,] \le \omega_{ICE\,MAX} \\ 0 \le \omega_{MG}(t) \le \omega_{MG\,MAX} \\ T_{ICE}[t, clutch_{state}(t) = 0\,] = 0 \\ T_{ICE\,min}[\omega_{ICE}(t))] \le T_{ICE}[t, clutch_{state}(t) = 1\,] \\ \le T_{ICE\,MAX}[\omega_{ICE}(t)] \end{gathered} \quad (12)$$

$$T_{MG_{min}}[\omega_{MG}(t)] \leq T_{MG}(t) \leq T_{MG_{MAX}}[\omega_{MG}(t)]$$

SOC constraints:

$$SOC(t_{end}) \geq SOC_{target}$$
$$\dot{SOC}(t) = f[SOC(t), \omega_{MG}(t), T_{MG}(t)]$$
$$SOC_{min} \leq SOC(t) \leq SOC_{MAX}$$

Parallel P2 HEV powertrain constraints:

$$\omega_{MG}(t) = \frac{v(t) \cdot \tau_{diff} \cdot \tau_{gear}[n_{gear}(t)]}{r_{wheel}}$$
$$\omega_{ICE}(t) = \omega_{MG}(t) \cdot clutch_{state}(t)$$
$$T_{MG}(t) = \left\{ \frac{T_{wheels}(t)}{\tau_{diff} \cdot \tau_{gear}[n_{gear}(t)] \cdot \eta_{driveline}^{sign[T_{wheels}(t)]}} - T_{ICE}(t) \right\}$$

Smooth HEV driving constraints:

$$T_{ICE}[t, T_{wheels}(t) < 0] = 0$$
$$\sum_{t=1}^{t_{end}} \left[\dot{m}_{fuel}(t) \neq \dot{m}_{fuel}(t-1)\right] \leq N_{cranking,MAX}$$
$$\sum_{t=1}^{t_{end}} \left[n_{gear}(t) \neq n_{gear}(t-1)\right] \leq N_{shifts,MAX}$$

The optimal plug-in HEV control problem aims at minimizing the overall fuel and electrical energy consumption while complying with various constraints. In this paper, specific costs are considered to weight fuel consumption and net electricity consumption. As consequence, the cost function to be minimized is represented by the overall economic cost of the trip $cost_{trip}$. $c_{fuel}$ and $c_{elec}$ stand for the fuel and electricity prices per unit, respectively. Their values have been selected here respectively as 1.41 euros per liter and 0.22 euros per kilowatt-hour, which relate to average prices observed in Italy in the first half of 2020 [33][34]. $\rho_{fuel}$ is the fuel density in grams per liter. The electrical energy consumption in kilowatt-hours can be evaluated in eq. (12) by multiplying the battery pack open-circuit voltage times current and dividing by 3.6e6. The total trip cost is representative of the plug-in HEV fuel and electrical energy consumption, and it can be evaluated as a function of the evolution of HEV control variables over time, including the gear engaged, the ICE torque and the clutch state. Mechanical constraints involve limiting the gear engaged within $n_{gear,MAX}$, i.e. the number of gears embedded in the AMT, and restricting the ICE and MG operating points within allowed physical regions. The evolution of battery SOC over time follows the numerical modeling approach reported in (8)-(10), while related constraints involve its value at the end of the driving mission being equal or above the set target $SOC_{target}$. Moreover, the instantaneous battery SOC should always be contained within allowed limits. Speed and torque of ICE and MG can be evaluated following parallel P2 HEV powertrain constraints as functions of values of control variables and external inputs (i.e. vehicle speed and torque request). Finally, retained smooth HEV driving constraints involve setting the ICE torque to 0 when the vehicle is decelerating (i.e. $T_{wheels} < 0$). Indeed, the noise caused by the ICE delivering positive torque might considerably compromise the riding perception when the driver intends to slow down to vehicle [35]. Moreover, the number of ICE cranking and gear shifting events in the overall driving mission should be limited below the predefined scalar thresholds $N_{cranking,MAX}$ and $N_{shifts,MAX}$, respectively. An ICE cranking event and a gear shift can be detected in those time instants in which the fuel consumption switches from zero to a positive value and the selected gear number does not match with the gear selected at the previous time instant, respectively.

Smooth driving constraints are set here to guide the control optimization algorithm to identify appropriate HEV control policies in terms of drivability and riding perception. Indeed, it is commonly known in the literature that HEV optimal control algorithms would operate frequent ICE activations and gear shifts when constraining the frequencies for these events is neglected [36][37].

### *3.2. Dynamic Programming*

Assuming complete a priori knowledge of future driving for the given cycle, the corresponding global optimal solution for the plug-in HEV control problem with smooth driving constrains can be identified according to the Bellman's principle of optimality [38]. Deterministic DP can be used in this context as a

popular technique to find global optimal HEV control trajectories [39][40]. Fig. 2 illustrates the workflow of the DP algorithm implemented in this paper, which corresponds to the one embedded in the generic DP Matlab® toolbox made available by Sundstrom and Guzzella [41]. In general, the optimal HEV control solution is identified by DP by exhaustively sweeping all possible discretized control actions while solving an optimization problem backwardly form the final time instant to the initial one of the considered driving mission [42][43]. Input parameters to the DP algorithm include in this case the numerical model of the HEV powertrain, the specific driving mission under analysis, $SOC_{target}$ and the battery SOC at the beginning of the driving mission. Details for the operating steps of the implemented DP algorithm are then provided as follows.

*Step A.* DP variables including control variable set, state variable set, cost-to-go-function and others are set in this step. The control variable set *U* associated to the HEV powertrain architecture considered here is shown in Eq. (13) and includes the gear number selection, the controlled torque of the ICE, and the controlled clutch state.

$$U = \begin{Bmatrix} n_{gear} \\ T_{ICE} \\ clutch_{state} \end{Bmatrix} \quad (13)$$

Combining control variables included in *U* allows generating all the possible discretized HEV control actions that comply with the constraints introduced in eq. (12).

DP requires the definition of the state variable set *X* as well that includes the variables that are monitored over time throughout the considered drive cycle in eq. (14) [44].

$$X = \begin{Bmatrix} SOC \\ n_{gear} \\ clutch_{state} \end{Bmatrix} \quad (14)$$

*X* comprises in this case the battery SOC which is tracked in order to allow avoiding excessive charge-depleting HEV operation, to comply with SOC constraints in eq. (12) and to properly evaluate SOC dependent battery parameters such as open-circuit voltage and internal resistance for example. The gear number $n_{gear}$ and the clutch state $clutch_{state}$ are included in *X* to detect gear-shifting and ICE de/activation events, respectively. Compliance with the introduced smooth HEV driving constraints is allowed in this way. Since the retained DP tool allows constraining final values of state variables, the battery SOC is set here to be within allowed limits at the end of each retained driving mission [44].

Finally, an instantaneous cost-to-go function $J_{DP}$ is considered as shown in eq. (15):

$$J_{DP}(t) = \left[c_{fuel} \cdot \frac{\dot{m}_{fuel}(t)}{\rho_{fuel}}\right] + \left\{c_{elec} \cdot \left[\frac{OCV_{pack}(t) \cdot I_{pack}(t)}{3.6e6}\right]\right\} + \mu_{ICE}[clutch_{state}(t) \neq clutch_{state}(t-1)] + \mu_{gear}\left[n_{gear}(t) \neq n_{gear}(t-1)\right] \quad (15)$$

where the first two terms respectively relate to fuel consumption cost and electrical energy consumption cost, while the latter two terms allow accounting for smooth driving conditions. $\rho_{fuel}$ is the fuel density in grams per liter. $\mu_{ICE}$ and $\mu_{gear}$ are constant penalization factors applied at each time instant in which gear shifting and ICE de/activation are

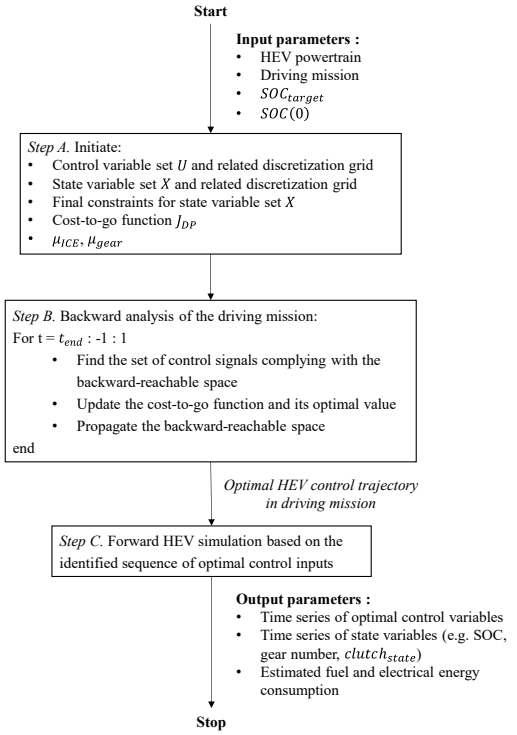


Fig. 2 Workflow of the DP algorithm for solving the optimal plug-in HEV control problem.

triggered, respectively. Both $\mu_{ICE}$ and $\mu_{gear}$ require calibration to ensure satisfaction of smooth driving constraints introduced in eq. (12) while avoiding excessive HEV fuel and electrical energy economy worsening. It should be noted that two further state variables could have been considered in DP to track over time the number of gear shifts and ICE de/activation events. Nevertheless, this approach would have remarkably further deteriorated the computational efficiency of the DP algorithm. Furthermore, the automated calibration of $\mu_{ICE}$ and $\mu_{gear}$ is not considered in the illustrated DP workflow since the computational efficiency of the algorithm would further decay, but rather a manual calibration of these coefficients will be performed in Section 5, and only the computational time associated to a single execution of the DP workflow illustrated in Fig. 2 will be considered. On the other hand, the next section will highlight how effective and computationally efficient calibration of similar coefficients for smooth HEV driving conditions can be achieved in the version of SERCA introduced here.

*Step B.* A backward analysis of the driving mission is performed from the last time instant to the initial one. At each time step, the discretized control variables that comply with the backward-reachable space are identified first. The backward-reachable space is a dynamic state constraint ensuring that the limitations imposed for the final values of state variables can be met. Then, the instantaneous cost-to-go function is updated for the discretized values of control and state variables within the backward-reachable space. The minimal value of the cumulated cost function up to the time instant under analysis is identified, and the corresponding control trajectory is selected as the optimal one. Finally, before moving to the previous time instant, the related backward-reachable space is propagated. This procedure is iterated until the initial time instant of the driving mission is reached, and the optimal HEV control trajectory over time can finally be identified. The interested reader can consult [45] for more details regarding this methodology.

*Step C.* A forward simulation of the plug-in HEV is performed by considering as input the optimal control trajectories previously computed. This allows evaluating both the time series of the HEV states, and the estimated fuel and electrical energy consumption in the overall driving mission.

The main drawback of DP relates to its conspicuous computational cost, which exponentially increases when considering further state variables due to curse of dimensionality [46]. A compelling need might therefore relate to identify computationally efficient near-optimal control strategies for plug-in HEVs considering smooth driving constraints. In the next section, the formulation of the SERCA algorithm for plug-in HEVs will be introduced to overcome this drawback.

## 4. SERCA formulation for plug-in HEVs considering smooth driving constraints

As it has been described earlier, an appropriate energy management strategy needs implementation to rapidly predict the fuel and battery energy consumption of plug-in HEV design options in electrified powertrain design tools. As regards SERCA, its successful implementation has been discussed so far for HEVs operating in charge-sustaining mode only, where the contribution of external battery electrical energy coming from the grid is not considered [28]. Nevertheless, when it comes to plug-in HEVs, numerical simulations are required to evaluate the operation of the electrified powertrain in charge-depleting mode as well, e.g. when the user starts the journey after charging the battery to the maximum allowed value of SOC. From a numerical point of view, this translates into considering different and broaden battery SOC intervals by retaining different constraints on the initial and final values of SOC. An adaptation of the previously introduced SERCA algorithm needs therefore development to account for these considerations. The workflow of the version of SERCA implemented for plug-in HEVs considering smooth driving constraints is illustrated in Fig. 3 and described in the follow-up of this section.

Concerning parallel P2 HEVs, the baseline SERCA algorithm for HEV charge-sustaining operation retains as input the illustrated numerical model of the electrified powertrain design candidate and the driving mission that the design engineer intends to consider. These input data are retained as well in the version of

SERCA updated for plug-in HEVs, while further input parameters are required. These include (1) the level of battery SOC at the beginning of the retained driving mission $SOC_0$ (as assumed by the vehicle designer); (2) the minimum level of battery SOC to be guaranteed at the end of the retained driving mission $SOC_{target}$ (as a criterion specified by the vehicle designer); (3) $N_{cranking,MAX}$ denoting the maximum number of ICE activations operable for the entire driving mission (as a criterion specified by the vehicle designer); (4) $N_{shifts,MAX}$ denoting the maximum number of gear shifts operable for the entire driving mission (as a criterion specified by the vehicle designer). Then, the workflow of the SERCA algorithm for PHEVs can be described as follows in eight steps:

*Step A.* Initial values are set for $\lambda_{ICE}$ and $\lambda_{GS}$ which denote constant operating parameters of SERCA for tuning the number of ICE activations and the number of gear shifts, respectively. Both $\lambda_{GS}$ and $\lambda_{ICE}$ are particularly set to 1 not to excessively penalize fuel and electrical energy consumption in the first iteration of the algorithm. A further parameter which initially needs definition in the version of the SERCA algorithm for plug-in HEVs is the number of sub-cycles $N_{sub-cyc}$, i.e. the number of portions of the retained driving mission which will be optimized by SERCA separately. As it will be explained in step H in the algorithm, dividing the entire driving mission in more sub-cycles enhances the capability of the plug-in HEV powertrain controlled by SERCA of respecting allowed SOC limits. At the beginning, the number of sub-cycles might be set to 1, i.e. the overall driving mission is considered at once.

*Step B.* The net consumable battery energy throughout the given driving mission in ampere-seconds is computed according to the set values of initial SOC and final SOC following eq. (16):

$$E_{batt} = \left[SOC(0) - SOC_{target}\right] \cdot Ah_{pack} \cdot 3600 \quad (16)$$

*Step C.* The workflow of the traditional version of SERCA is performed for each sub-cycle of the retained driving mission, as reported in Algorithm 1 in [28]. The three main stages of SERCA are thus executed, namely the sub-problems exploration, the optimal operating points definition and the energy balance realization. As a general reminder, in SERCA optimal operating points at each time instant of the driving missions are the ones maximizing a slope parameter which is the ratio between charged battery energy and fuel consumed by the ICE. In the energy balance achievement step, the initial criterion of iterating the algorithm until the value of $E_{EV}$ is greater than 0 is replaced by the recursive execution of the electric-to-hybrid replacement process until the value of $E_{EV}$ is greater than $E_{batt}$ in order to account for charge-depleting operation of plug-in HEVs. In this framework, the lower the values of $\lambda_{ICE}$ and $\lambda_{GS}$, the more priority will be given by SERCA to respectively reduce the number of ICE activations ad gear shifts at the expenses of worsening estimated fuel economy [28]. The aim of introducing $\lambda_{ICE}$ and $\lambda_{GS}$ can be compared to the use of $\mu_{ICE}$ and $\mu_{gear}$ in DP and to the use of co-states in the PMP for regulating changes in corresponding vehicle states over time. These coefficients need tuning to meet the retained smooth HEV driving constraints according to the driving mission and the starting SOC. To this end, the proved computational efficiency of SERCA is remarkably advantageous compared with DP. When multiple sub-cycles are retained for the driving mission under analysis, the value of $E_{batt}$ is updated at each sub-cycle following eq. (16) and retaining the final value of SOC for the previous sub-cycle as $SOC(0)$. Moreover, a check is conducted before considering each sub-cycle whether the plug-in HEV operation reached the charge-sustaining criterion during the previous sub-cycle. This corresponds to the final value of battery SOC for the previous sub-cycle being around $SOC_{target}$. In this case, since the contribution of the net battery energy coming externally from the grid has been depleted, the SERCA algorithm for the present sub-cycle is iterated until the value of $E_{EV}$ is greater than 0 to account for charge-sustaining operation.

*Step D.* During Step C, an assumption is typically made in SERCA that the battery parameters (i.e. $OCV_{pack}$ and $R_{pack}$) do not vary according to the instantaneous value of SOC. A globally optimal control solution could be achieved in the literature while considering this assumption in case of HEV charge-sustaining operation [47]. However, when dealing with charge-depleting operation of plug-in HEVs, the value of SOC throughout the same driving mission might span a wider range of values entailing higher variations in the values of battery internal

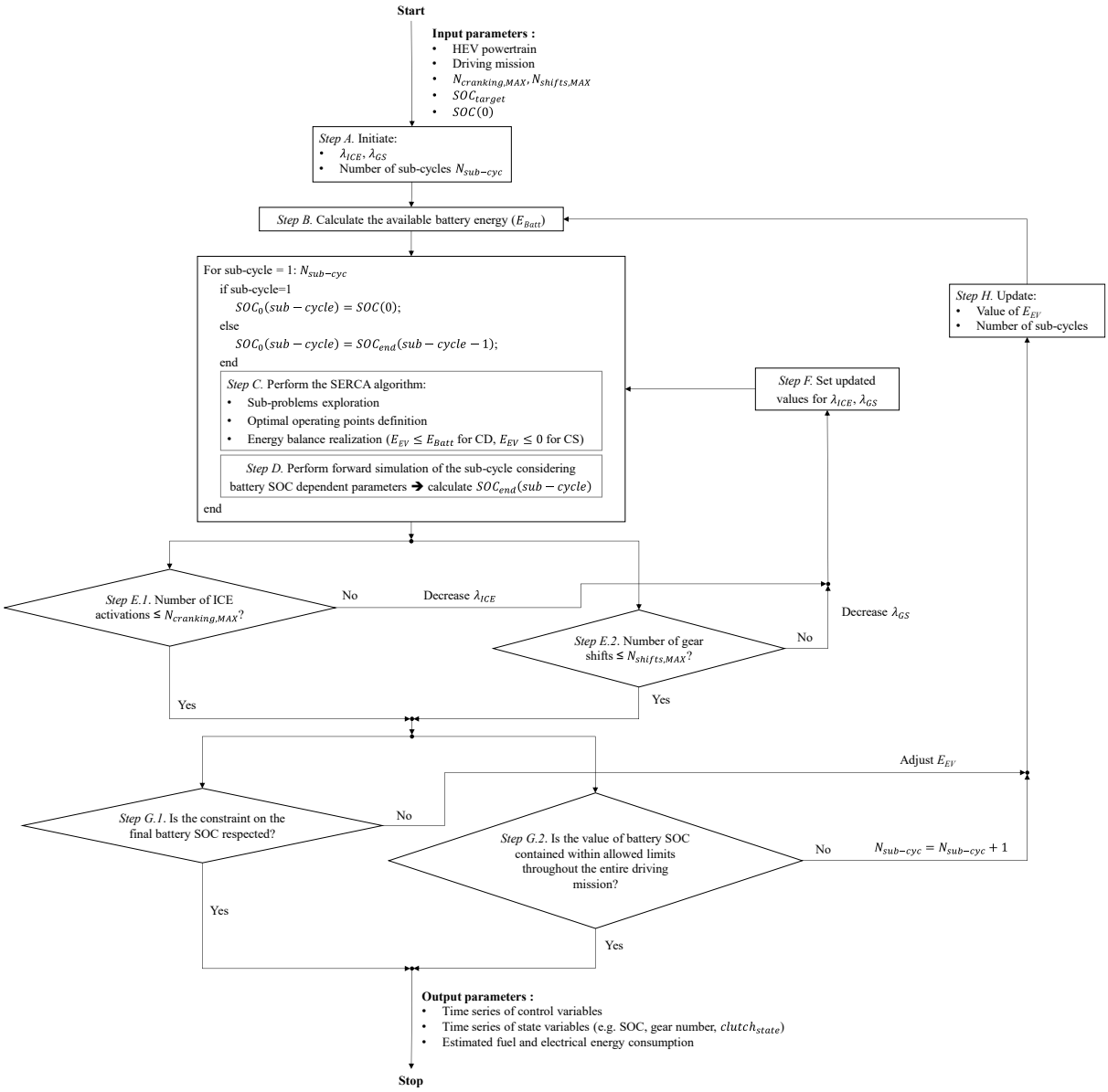


Fig. 3 Workflow of the SERCA algorithm applied to plug-in HEVs considering smooth HEV driving constraints.

resistance and open-circuit voltage, thus potentially compromising the solidity of this hypothesis. Fig. 4 illustrates a comparison between time series of battery SOC in the worldwide harmonised light-vehicle test procedure (WLTP) respectively evaluated according to an HEV forward model and to an HEV model with constant battery parameters such as the one considered in Step C of SERCA. The starting battery SOC is 95%, and the potential SOC estimation error is illustrated as well in Fig. 4. The estimation error is proved to cumulate over time throughout WLTP achieving a remarkable 90% peak. Partitioning the entire driving mission in more sub-cycles allows mitigating this issue. Moreover, an additional step is executed to

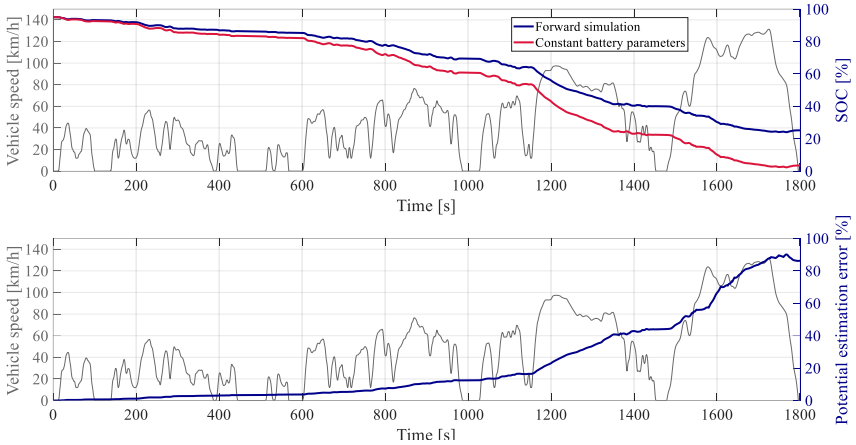


Fig. 4. Time series of battery SOC in WLTP evaluated according to HEV forward model and to HEV model with constant battery parameters, along with time series of potential SOC estimation error in WLTP.

completely overcome this potential drawback: after the workflow of the traditional SERCA algorithm has been completed in Step C, a forward simulation is performed for each sub-cycle while considering the dependency of battery parameters (i.e. internal resistance and open-circuit voltage) from the instantaneous value of battery SOC. To this end, time series of control variables (i.e. $n_{gear}$, $T_{ICE}$ and $clutch_{state}$) are fed as input into the HEV powertrain numerical model described in Section 2. This allows determining the battery energy consumption and the overall SOC trajectory over time (including its final value) more accurately for each sub-cycle. It should be reminded that the simulation of the entire driving mission is performed by iteratively executing Step C and Step D for each sub-cycle according to the described procedure before moving to Step E. Moreover, the values of $\lambda_{ICE}$ and $\lambda_{GS}$ selected in Step A or in Step F are kept constant throughout the iterative analysis of each sub-cycle in Step C and Step D.

*Step E*. Once all the sub-cycles of the retained driving mission have been analyzed and simulated according to SERCA, a check is conducted for both the number of ICE activations and gear shifts being less or equal than $N_{cranking,MAX}$ and $N_{shifts,MAX}$, respectively. Step F is executed in negative case, while the algorithm skips directly to step G in positive case. The values of $N_{cranking,MAX}$ and $N_{shifts,MAX}$ can be set arbitrarily by the HEV designer according to engineering experience or predefined HEV development targets imposed by given sub-components of the electrified powertrain. As example, the AMT under development might not be able to perform a certain amount of gear shifts over time due to excessive and hazardous mechanical stress.

*Step F*. In case either the number of ICE activations or the number of gear shifts exceed the limits set by the designer for the retained driving mission, $\lambda_{ICE}$ or $\lambda_{GS}$ are respectively decreased to allow the SERCA algorithm improving the drivability of the PHEV powertrain design candidate under analysis. Steps C, D, E and F are particularly iterated until the smooth HEV driving requirements reported in eq. (12) and imposed by the designer in terms of maximum number of ICE activations and gear shifts over time are fulfilled.

*Step G*. A further two-stage check is performed concerning the battery SOC trajectory generated by the forward simulations performed at step D considering battery SOC dependent parameters. A first check is conducted on $SOC_{end-SERCA}$. i.e. the value of battery SOC achieved at the end of the considered driving mission according to SERCA. This should be particularly equal or higher than $SOC_{target}$ as specified by the designer and reported in eq. (12). A second inquiry regards the overall SOC trajectory in the driving mission, whose value should never be

higher than the maximum SOC allowed by the battery nor lower than the minimum SOC allowed by the battery. If both conditions are satisfied, the SERCA algorithm for plug-in HEVs is concluded, otherwise step H is executed.

*Step H*. In case an unsatisfactory value of SOC at the end of the retained driving mission $SOC_{end-SERCA}$ is achieved due to the assumption of constant battery parameters (e.g. lower than $SOC_{target}$), an update is performed regarding the value of $E_{batt}$. Assuming that the generic iteration *j* of SERCA has been performed for the given driving mission, the updated value of $E_{batt}$ in ampere-seconds at the following iteration *j+1* can be computed using eq. (17).

$$E_{batt_j+1} = E_{batt_j} + \left(SOC_{end-SERCA} - SOC_{target}\right) \cdot Ah_{pack} \cdot 3600 \quad (17)$$

This allows the SERCA algorithm achieving a value of SOC at the end of the driving mission closer to the target $SOC_{target}$ in the following iteration *j+1*. In general, the SERCA algorithm enables complying with the allowed value of net battery energy consumption by fulfilling an energy balance regarding the overall driving mission under analysis. This allows preserving computational rapidness for performing the overall algorithm. However, the instantaneous SOC value throughout the considered driving mission is not strictly considered in the SERCA optimization process. Especially when analyzing driving missions with considerably long distance, it might happen that the punctual value of SOC resulting from the electrified powertrain operation set by SERCA exceeds the minimum or maximum allowed value. Increasing the number of considered sub-cycles $N_{sub-cyc}$ for the given driving mission may allow overcoming this drawback. As example in charge-sustaining operation, the battery SOC is required to converge to the target $SOC_{target}$ at the end of each sub-cycle, thus increasing the overall restrictions imposed to the used SOC window. However, refining the division of the entire driving mission in more sub-cycles might potentially compromise the fuel economy capability of the retained PHEV. For this reason, the entire driving mission is considered at once in the first iteration of SERCA, while the segmentation into progressively more sub-cycles is executed only in case the battery SOC constraints are not fulfilled. Steps B to H are thus repeated until all the smooth HEV driving criteria and battery SOC criteria are not satisfied at once by the plug-in HEV control solution identified by SERCA.

Once the described workflow of SERCA is completed, obtained output parameters include time series of control variables (i.e. gear number, ICE torque and clutch state), time series of state variables (e.g. battery SOC), and estimated fuel and electrical energy consumption for the retained plug-in HEV performing the retained driving mission.

## 5. Results – case study

This section aims at presenting a case study that assesses the effectiveness of the proposed version of SERCA for plug-in HEVs. The parallel P2 PHEV data retained in this case are reported in Table 1, where the vehicle chassis data relate to an A-segment passenger car from the US EPA database [48]. The ICE data is for a 3 cylinder in-line naturally aspired spark-ignition engine, while the size of the interior permanent magnet MG has been determined in order to get a hybridization factor of around 35%. The operating map for the ICE has been generated by means of Amesim® software and is illustrated in Fig. 5 [49]. Similarly, a lookup table for the MG efficiency of an interior permanent magnet synchronous electric machines has been derived in Amesim® software according to the procedure reported in [50] and it is illustrated in Fig. 5. The battery pack has been modeled as consisting of quantity 400 A123 26650 cells in 100S 4P configuration, thus achieving a nominal capacity of 3.04kWh. Values of pen-circuit voltage and internal resistance as function of battery SOC have been retained from [51] considering new cell conditions. Such limited capacity selected for the battery pack of the representative plug-in HEV can be justified first with the small size of the considered A-segment passenger car. Indeed, embedding a larger battery pack, typical of current plug-in HEVs, might introduce packaging issues when trying to fit both the battery pack and the hybrid electric powertrain in the limited volume allowed by an A-segment passenger car. Moreover, downsizing the battery pack might evidently involve considerable benefits from the retail

Table 1
Plug-in HEV data used for SERCA validation

| Component | Parameter | Value |
|---|---|---|
| Vehicle | Mass | 1002 Kg |
| | $RL_A$ | 104.49 N/m |
| | $RL_B$ | 2.43 N/(m/s) |
| | $RL_C$ | 0.41 N/(m/s$^2$) |
| | Wheel dynamic radius ($r_{wheel}$) | 0.317 m |
| ICE | Capacity | 1.0 L |
| | Configuration | 3 cylinders, in-line |
| | Type | Spark ignition, naturally aspired |
| | Maximum power | 51 kW @ 6000 rpm |
| | Maximum torque | 92 Nm @ 3500 rpm |
| | $\rho_{fuel}$ | 749.5 g/L |
| Transmission | Gear ratios | [3.85 ; 2.27 ; 1.52 ; 1 ; 0.81] |
| | Efficiency ($\eta_{driveline}$) | 0.90 |
| Final drive | Gear ratio | 3.70 |
| MG | Maximum power | 28 kW |
| | Maximum torque | 91 Nm |
| Auxiliaries | Electrical subsystem power | 500 W |
| Battery pack | Configuration | 100S 4P |
| | Nominal capacity | 3.04 kWh |
| | Cell type and capacity | A123 ANR26650M1-B, 2.5Ah |

price point of view. Finally, a downsized battery pack increases the probability of using hybrid electric mode more than only pure electric mode in everyday driving missions. This allows numerically testing more thoroughly and exhaustively the effectiveness of the HEV control algorithms retained in this case study. Transmission data reported in Table 1 correspond to a five-speed AMT.

Two driving missions are particularly considered in this case study represented by the WLTP and a real-world driving mission (RWC) for which time series for vehicle speed and road altitude are shown in Fig. 6. RWC particularly refer to a journey around 72 kilometres long that includes different driving

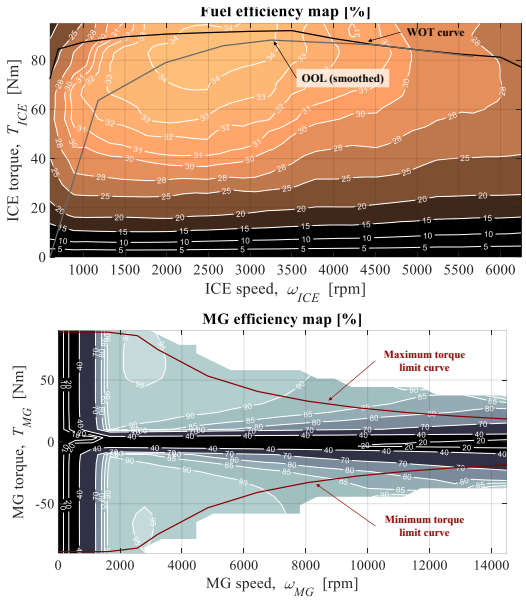


Fig. 5. Generated 1.0 L 3 cylinders in-line 51 kW engine efficiency map and interior permanent magnet 28 kW electric motor efficiency map.

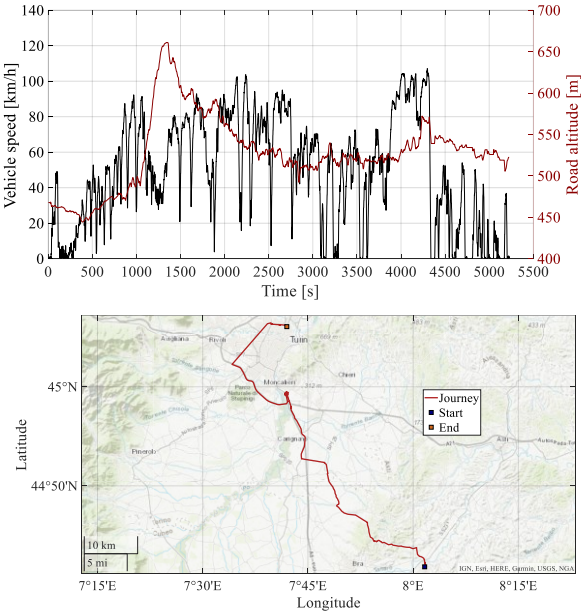


Fig. 6. Vehicle speed profile, road altitude profile and geographic map for the real-world driving mission (RWC) recorded through global positioning system.

conditions such as urban, extra-urban, highway, uphill and downhill. The duration for RWC is around 1.5 hours and it has been recorded by means of global positioning system in Piedmont, northern Italy, as illustrated in Fig. 6. Road altitude has been recorded as well over time while performing RWC in Fig. 6. Compared with the WLTP, the simulation of RWC is thus more representative of real-world driving conditions. From a numerical modeling perspective, changes in road altitude over time allow evaluating the road slope angle $\vartheta$, which was in turn used in eq. (3) to calculate the vehicle resistive force due to road slope.

In order to thoroughly evaluate the plug-in HEV operation, simulations for both WLTP and RWC are performed considering different values of battery SOC when starting the driving mission, particularly corresponding to 95% (i.e. battery charged to the maximum allowed value), 80%, 60%, 40% and 25%. The value of $SOC_{target}$ is set to 25% in this case. All the retained starting SOC cases are considered for the plug-in HEV performing the two driving missions and being controlled off-line by both SERCA and DP. This allows thoroughly validating the near optimality of SERCA when the net battery energy use over the driving mission change due to the different starting SOC. Moreover, the robustness of the calibration procedure of $\lambda_{ICE}$ and $\lambda_{GS}$ in SERCA can be validated in this way for different values of starting SOC. As example, the ICE needs to be switched on more frequently and to be kept activated for longer as the value of starting SOC decreases. In this context, the value of $\lambda_{ICE}$ needs to be fine-tuned for preserving both the compliance with smooth driving constraints and the near optimality of the fuel and electrical energy economy assessed.

Minimum and maximum allowed values of battery SOC throughout the overall driving missions are assumed being 8% and 95%, respectively. The control variable related to $T_{ICE}$ is discretized with a step of 5 Nm [39], while 1,000 points are retained for discretizing the SOC state variable in each DP simulation [29]. Values of $N_{cranking,MAX}$ and $N_{shifts,MAX}$ set here depend on the duration of the specific driving mission and are reasonably assumed being 15 and 135 per 30 minutes of driving, respectively. Setting limits for $N_{cranking,MAX}$ and $N_{shifts,MAX}$ challenges the HEV control algorithms to comply with additional smooth driving constraints. At present, iterated executions of the algorithms are therefore required to find the optimised HEV control solution in terms of fuel and electrical energy economy while complying with smooth driving constraints. Computational efficiency is a key feature to efficiently iterate the control algorithm and thus meet smooth driving constraints. As it will be illustrated below, SERCA remarkably outperforms DP in terms of computational efficiency.

Simulations have been performed here in MATLAB® software and considering a desktop computer with Intel Core i7-8700 (3.2 GHz) and 32 GB of RAM. Once the entire workflow of SERCA for plug-in HEVs illustrated in Fig. 3 is completed for a simulation case, the same simulation has been repeated considering DP as energy management strategy and manually tuning weighting factors for the number of ICE activations and gear shifts until HEV performance complying with imposed requirements and comparable with SERCA was achieved. On one hand, this procedure allows performing a straightforward comparison of obtained results between SERCA and DP under similar drivability constraints. On the other hand, it should be noted that presented results in terms of computational time for DP will consider only a single simulation, i.e. discarding the eventual previous attempts not fulfilling smooth driving criteria.

Table 2 and Table 3 report obtained results in terms of predicted fuel consumption, electrical energy consumption, estimated plug-in HEV operative cost, number of ICE activations, number of gear shifts and computational time for both SERCA and DP in WLTP and RWC, respectively. Fuel consumption, electrical energy consumption, and estimated plug-in HEV operative cost have been particularly weighted over 100 kilometers considering the spatial distance covered in the corresponding driving mission. Furthermore, time series for battery SOC, gear number and cumulated fuel consumption for all the considered starting SOC cases in the two retained driving missions are illustrated in Fig. 7 and in Fig. 8, respectively. Overall, obtained results suggest that the near-optimality of the fuel and electrical energy economy predicted by SERCA and weighted according to the specific costs might be preserved for

Table 2

Results for fuel consumption, number of ICE activations, number of gear shifts and computational time for the plug-in HEV controlled by SERCA and DP in WLTP

| Starting SOC [%] | Algorithm | Fuel consumption [L/100 km] | Electrical energy consumption [kWh/100 km] | Plug-in HEV operative cost [€/100 km] | ICE activations | Gear shifts | Computational time [min] |
|---|---|---|---|---|---|---|---|
| 95 | SERCA | 1.51 | 9.03 | 4.12 (+0.9%) | 4 | 89 | 0.3 (-99.9%) |
| | DP | 1.51 | 8.89 | 4.08 | 6 | 74 | 242.8 |
| 80 | SERCA | 2.11 | 7.09 | 4.53 (+1.0%) | 10 | 89 | 0.3 (-99.8%) |
| | DP | 2.09 | 6.96 | 4.48 | 5 | 76 | 202.5 |
| 60 | SERCA | 2.94 | 4.48 | 5.13 (+1.6%) | 10 | 89 | 0.3 (-99.9%) |
| | DP | 2.90 | 4.39 | 5.05 | 8 | 75 | 269.4 |
| 40 | SERCA | 3.81 | 1.91 | 5.79 (+2.6%) | 12 | 89 | 0.3 (-99.9%) |
| | DP | 3.71 | 1.86 | 5.64 | 11 | 80 | 214.0 |
| 25 | SERCA | 4.51 | -0.02 | 6.35 (+4.4%) | 13 | 89 | 0.4 (-99.8%) |
| | DP | 4.32 | -0.03 | 6.09 | 13 | 78 | 345.2 |

Table 3

Results for fuel consumption, number of ICE activations, number of gear shifts and computational time for the plug-in HEV controlled by SERCA and DP in RWC

| Starting SOC [%] | Algorithm | Fuel consumption [L/100 km] | Electrical energy consumption [kWh/100 km] | Plug-in HEV operative cost [€/100 km] | ICE activations | Gear shifts | Computational time [min] |
|---|---|---|---|---|---|---|---|
| 95 | SERCA | 2.95 | 2.95 | 4.81 (+5.8%) | 36 | 327 | 1.1 (-99.9%) |
| | DP | 2.82 | 2.63 | 4.55 | 44 | 288 | 693.9 |
| 80 | SERCA | 3.17 | 2.31 | 4.98 (+5.6%) | 37 | 327 | 0.8 (-99.9%) |
| | DP | 3.01 | 2.12 | 4.71 | 37 | 322 | 643.7 |
| 60 | SERCA | 3.45 | 1.46 | 5.19 (+6.5%) | 36 | 327 | 0.8 (-99.9%) |
| | DP | 3.23 | 1.42 | 4.87 | 39 | 349 | 649.8 |
| 40 | SERCA | 3.69 | 0.62 | 5.42 (+6.8%) | 44 | 327 | 1.8 (-99.7%) |
| | DP | 3.51 | 0.61 | 5.08 | 41 | 384 | 618.3 |
| 25 | SERCA | 3.90 | -0.01 | 5.58 (+5.3%) | 44 | 327 | 2.1 (-99.9%) |
| | DP | 3.76 | -0.01 | 5.30 | 35 | 347 | 1475.4 |

this version of the algorithm dedicated to plug-in HEVs. This relate to the increase in plug-in HEV operative cost estimated by SERCA being always less than 4.4% and 6.8% compared with DP for WLTP and a long-distance real-world driving mission such as RWC, respectively. A slight increase in the percentage deviation of fuel economy between SERCA and DP can be observed compared with the correlative results previously shown for a parallel P2 HEV in terms of fuel economy solely. This minor drawback might relate to the implemented approach for calibrating the values of $\lambda_{ICE}$ and $\lambda_{GS}$ and in SERCA. While a brute force approach was adopted in [28] in exploring all the possible values for these coefficients, an iterative methodology is implemented in this paper that enables updating the values for these two coefficients only until the smooth drivability requirements are fulfilled in step E and step F of Fig. 3. On its behalf, the updated approach for calibrating $\lambda_{ICE}$ and $\lambda_{GS}$ contributes to further increase savings in the computational time for SERCA: on average 0.3 minutes are required to simulate the parallel P2 plug-in HEV in WLTP using SERCA here, while around 2.4 minutes were required to perform the same task on the same computational

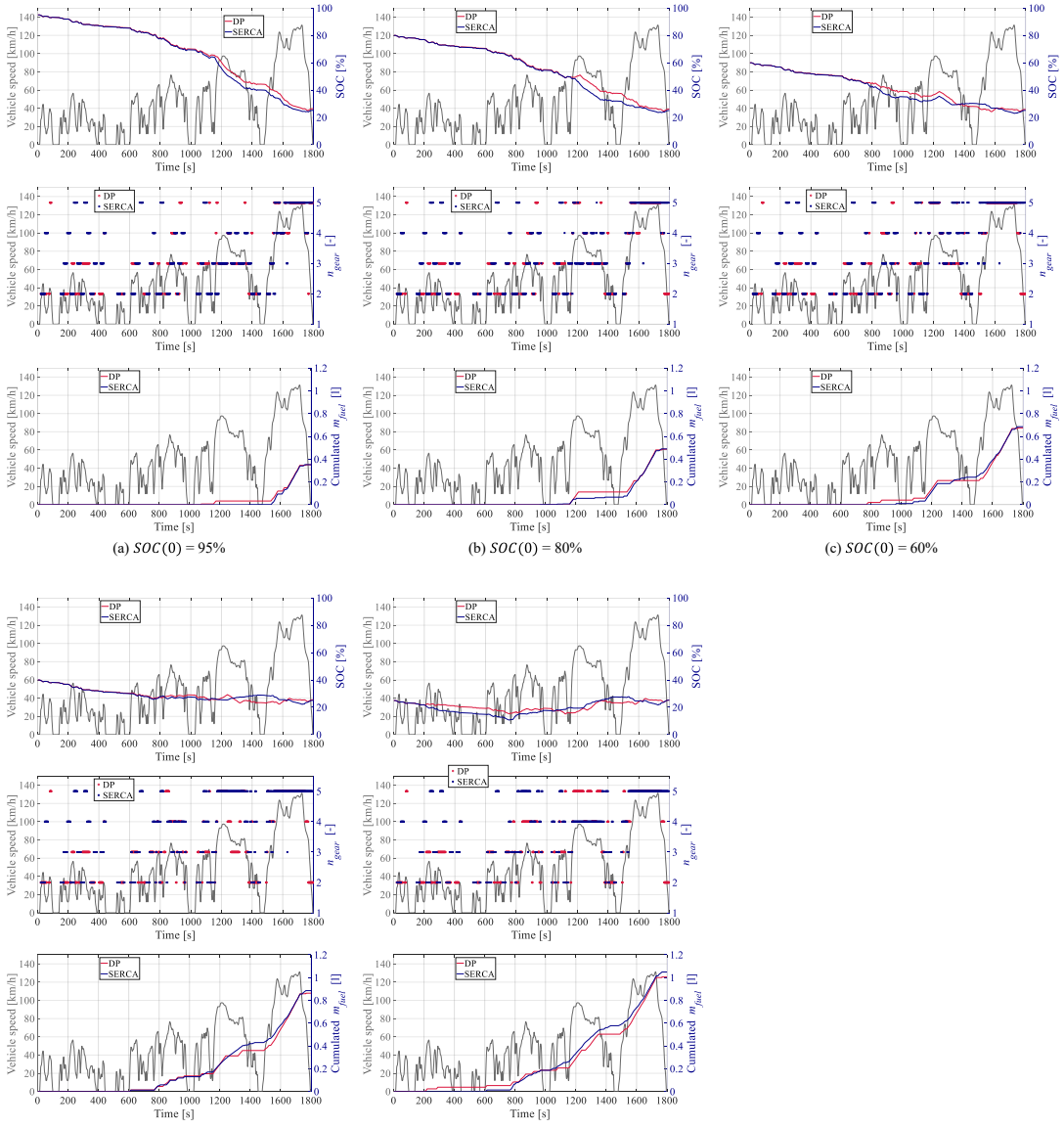


(a) $SOC(0) = 95\%$ (b) $SOC(0) = 80\%$ (c) $SOC(0) = 60\%$

(d) $SOC(0) = 40\%$ (e) $SOC(0) = 25\%$

Fig. 7 Battery SOC, gear number and predicted fuel consumption for the plug-in HEV controlled by SERCA and DP in WLTP for different values of starting battery SOC.

device in [28]. This is a further advantage in computational light-weighting since, compared with DP, lower computational times by around 99.9% are required by SERCA to complete both WLTP and RWC. It should be reminded that the computational time reported for DP does not account for the tuning process of $\mu_{ICE}$ and $\mu_{gear}$. If the calibration of these two coefficients was considered, the overall computational time for DP would remarkably further increase. As it can be noticed in Table 2 and in Table 3, smooth driving constraints imposed on the number of ICE activations and gear shifts can be satisfied thanks to the implemented plug-in HEV control approach. Moreover, as illustrated in Fig. 7 and in Fig.

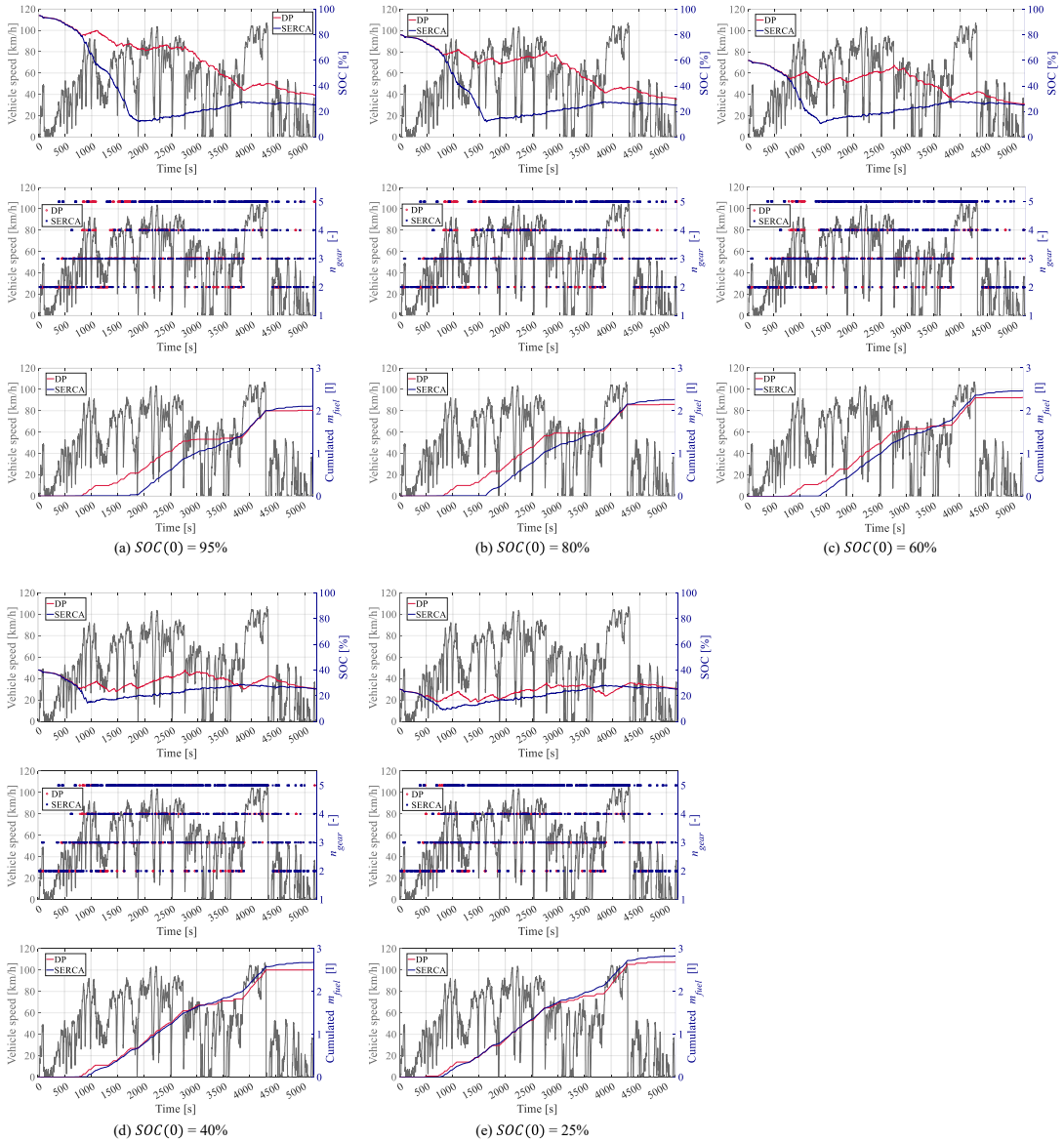


(a) $SOC(0) = 95\%$ (b) $SOC(0) = 80\%$ (c) $SOC(0) = 60\%$

(d) $SOC(0) = 40\%$ (e) $SOC(0) = 25\%$

Fig. 8 Battery SOC, gear number and predicted fuel consumption for the plug-in HEV controlled by SERCA and DP in RWC for different values of starting battery SOC.

8, the final value of SOC never falls below the minimum allowed value $SOC_{target}$, thus corroborating the effectiveness of the proposed HEV control approach. Particularly for DP, the value of battery SOC at the end of the driving mission may exhibit slightly larger values compared with $SOC_{target}$ due to the interpolation within the discretized grid of the corresponding state variable.

Table 4 reports obtained results for the automated calibration of $\lambda_{ICE}$ and $\lambda_{GS}$ in SERCA based on the selected driving mission and the starting battery SOC value. Different values are obtained for both these coefficients in each simulation case, which motivates

Table 4

Calibrated values of $\lambda_{ICE}$ and $\lambda_{GS}$ for the plug-in HEV controlled by SERCA in WLTP and in RWC as function of different values of starting battery SOC

| Starting SOC [%] | $\lambda_{ICE}$ | | $\lambda_{GS}$ | |
|---|---|---|---|---|
| | WTLP | RWC | WTLP | RWC |
| 95 | 1.000 | 0.840 | 0.995 | 0.955 |
| 80 | 1.000 | 0.860 | 0.990 | 0.960 |
| 60 | 0.950 | 0.860 | 0.980 | 0.960 |
| 40 | 0.900 | 0.860 | 0.970 | 0.960 |
| 25 | 0.600 | 0.880 | 0.910 | 0.965 |

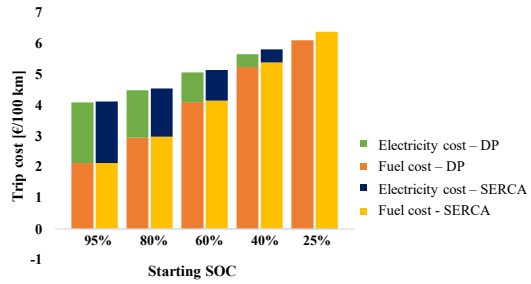


(a) WLTP

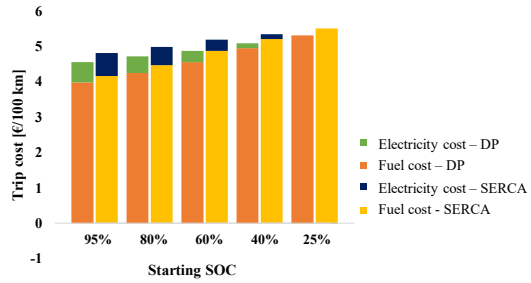


(b) RWC

Fig. 9. Predicted plug-in HEV trip cost in terms of fuel and electrical energy consumption for WLTP and RWC as predicted by SERCA and DP depending on the starting battery SOC.

the need for a calibration procedure in the SERCA algorithm for complying with the predefined smooth driving constraints depending on the driving mission and the starting battery SOC.

Finally, Fig. 9 illustrates the trip costs related to fuel and electrical energy consumption as predicted by SERCA and DP for both WLTP and RWC as a function of the starting battery SOC. A graphical representation of the near optimality of the HEV control solution identified by SERCA in terms of economic costs entailed by fuel and electrical energy consumption is provided in this way. Moreover, the economic viability of the electrical energy coming from the grid and stored in the battery of the plug-in HEV is proved in Fig. 9 considering the costs of the propelling energy. Indeed, 13.8% and 14.2% cost savings can be achieved by the plug-in HEV respectively controlled by SERCA and DP when starting the RWC with the battery fully charged compared with the related 25% starting SOC case. Corresponding potential economic savings for the WLTP further increase up to 35.1% and 33.0% for SERCA and DP, respectively. This relates to the limited kilometrical distance covered in WLTP compared with the RWC, which leverages the economic savings entailed by the increased use of electrical energy coming from the grid.

## 6. Conclusions

This work introduces a computationally efficient energy management approach for plug-in HEVs. An adaptation of the SERCA algorithm introduced in [28] that can optimally control plug-in HEVs at various level of battery SOC at the beginning of each driving mission is particularly discussed. The performance of the SERCA algorithm is validated by benchmarking with the global optimal HEV control reference provided by DP in terms of estimated operative costs derived by fuel and electrical energy consumption and computational cost in both a standard drive cycle and in a real-world long-distance driving mission. Other than minimizing the estimated fuel and electrical energy consumption, both control approaches aim at generating smooth hybrid supervisory control patterns by appropriately limiting the number of ICE activations and gear shifts over time. The SERCA algorithm has been demonstrated capable of simulating the near-optimal smooth driving constrained operation of a plug-in HEV in a 1.5 hour-long real-world driving mission in less than 2 minutes on a desktop computer. On the other hand, DP would require more than 10 hours to perform the same task without straightforwardly guaranteeing the satisfaction of smooth driving constraints retained. It

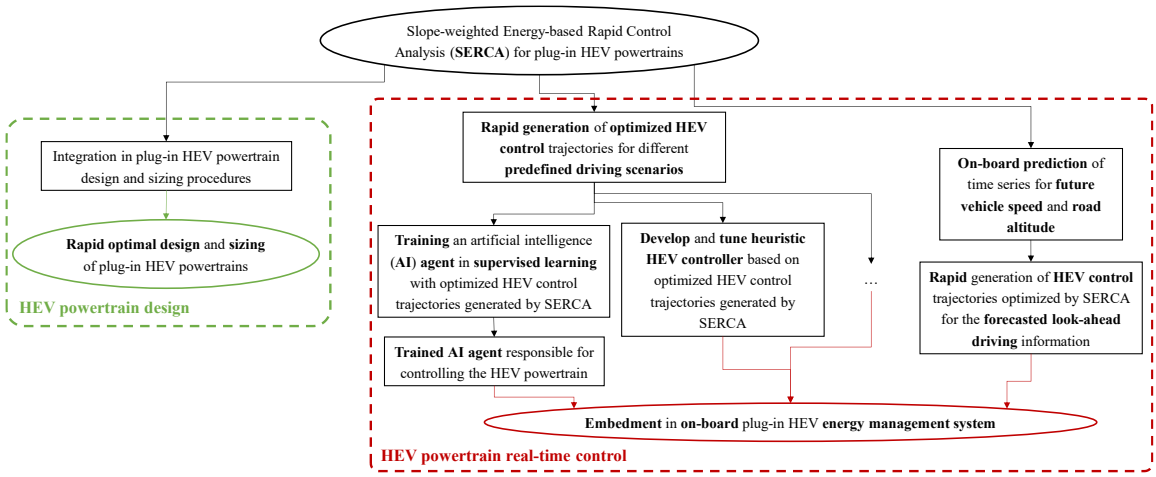


Fig. 10. Directions for future employment and practical application of the presented SERCA algorithm for plug-in HEVs in the domains of HEV powertrain design and real-time control.

should be admitted that implementing SERCA entails a slight increase in estimated fuel and electrical consumption compared with DP. However, this increment was proved being contained within few percentage points only.

The computational rapidness of SERCA and its near optimality in terms of estimated fuel and electrical energy consumption as illustrated in this paper open new possibilities for plug-in HEV powertrain design and on-board control. Fig. 10 outlines possible future developments of the SERCA algorithm for plug-in HEVs. Regarding HEV powertrain design, engineers could implement it to easily estimate the fuel and electrical energy economy capability of a given plug-in HEV powertrain layout. Computational efficiency can be enhanced in this way when exploring the large design space associated to plug-in HEV powertrain, while including for example the consideration of other vehicle states (e.g. battery state-of-health, battery temperature, after treatment system temperature) and the simulation of several long-distance real-world driving missions [52][53].

Moreover, future work could consider implementing SERCA in on-board plug-in HEV energy management systems. Indeed, computational efficiency is a major drive to foster effectiveness and affordability of vehicle on-board control units. A first possibility shown in Fig. 10 in this case relates to generate a large database of optimized HEV control trajectories considering different real-world driving scenarios. This can be performed rapidly thanks to the use of SERCA. Then, an artificial intelligence agent could be trained off-line in supervised learning mode to learn the optimized HEV control behaviour provided by SERCA. The trained artificial intelligence agent could then be embedded in the on-board plug-in HEV energy management system. Alternatively, the generated database of HEV control trajectories optimized by SERCA could be used to develop and tune heuristic HEV controllers. Further options are possible and could be explored in this framework in Fig. 10. For example, SERCA could be combined with recent advances in intelligent transportation systems and future velocity predictors to rapidly generate near-optimal plug-in HEV control trajectories based on the prediction provided in terms of vehicle speed and road altitude according to gathered look-ahead information [54][55]. The predicted control trajectories could then be applied by the on-board plug-in HEV energy management system that operates as a predictive controller.

## References

[1] Emadi A., “Transportation 2.0”, IEEE Power Energ Mag 2011;9(4):18–29.
[2] O. Andersson, P. Börjesson, “The greenhouse gas emissions of an electrified vehicle combined with renewable fuels: Life

cycle assessment and policy implications", Applied Energy 2021; 289: 116621.
[3] V. Keller, J. English, J. Fernandez, C. Wade, M. Fowler, S. Scholtysik et al., "Electrification of road transportation with utility controlled charging: A case study for British Columbia with a 93% renewable electricity target", Applied Energy 2019, vol. 253, no. 113536.
[4] Mortensen A. W., Mathiesen B. V., Hansen A. B., Pedersen S. L., Grandal R. D., Wenzel H., "The role of electrification and hydrogen in breaking the biomass bottleneck of the renewable energy system – A study on the Danish energy system", Applied Energy 2020, vol. 275, no. 115331.
[5] Anselma P.G., Belingardi G., "Next generation HEV powertrain design tools: roadmap and challenges", SAE Technical Paper 2019–01-2602 2019.
[6] Dimitrova Z., Maréchal F., "Techno–economic design of hybrid electric vehicles and possibilities of the multi-objective optimization structure", Applied Energy 2016, vol. 161, pp. 746-759.
[7] W. Zhuang, S.L. Eben, X. Zhang, D. Kum, Z. Song, G. Yin, J. Ju, "A survey of powertrain configuration studies on hybrid electric vehicles", Applied Energy 2020; 262: 114553.
[8] P. Wolfram, T. Wiedmann, "Electrifying Australian transport: Hybrid life cycle analysis of a transition to electric light-duty vehicles and renewable electricity", Applied Energy 2017, vol. 206, pp. 531-540.
[9] R.T. Doucette, M.D., McCulloch, "Modeling the prospects of plug-in hybrid electric vehicles to reduce CO2 emissions", Applied Energy 2011; 88(7): 2315-23.
[10] Peng W., Yang J., Lu X., Mauzerall, D. L., "Potential co-benefits of electrification for air quality, health, and CO2 mitigation in 2030 China", Applied Energy 2018, vol. 218, pp. 511-519.
[11] Ebrahimi S., Mac Kinnon M., Brouwer J., "California end-use electrification impacts on carbon neutrality and clean air", Applied Energy 2018, vol. 213, pp. 435-449.
[12] Zhou X., Qin D., Hu J., "Multi-objective optimization design and performance evaluation for plug-in hybrid electric vehicle powertrains", Applied Energy 2017, vol. 208, pp. 1608-1625.
[13] Eifler G., Dau A., Wetscher M., "Are hybrid-powertrains the right solutions to meet the EU-emission-targets 2030?", 20. Internationales Stuttgarter Symposium 2020, Proceedings, Springer Vieweg, Wiesbaden.
[14] Khanna N., Fridley D., Zhou N., Karali N., Zhang J., Feng W., "Energy and CO2 implications of decarbonization strategies for China beyond efficiency: Modeling 2050 maximum renewable resources and accelerated electrification impacts", Applied energy 2019, vol. 242, pp. 12-26.
[15] ] Biswas A, Emadi A., "Energy management systems for electrified powertrains: stateof-the-art review and future trends", IEEE Trans Veh Technol 2019;68(7):6453–67.
[16] Ngo V., Hofman T., Steinbuch M. and Serrarens, A., "Effect of gear shift and engine start losses on energy management strategies for hybrid electric vehicles", *Int. J. Powertrains* 2015; 4(2): 141–162.
[17] Yang Y., Hu X., Pei H., Peng Z., "Comparison of power-split and parallel hybrid powertrain architectures with a single electric machine: Dynamic programming approach", Applied energy 2016, vol. 168, pp. 683-690.
[18] Peng J., He H., Xiong R., "Rule based energy management strategy for a series–parallel plug-in hybrid electric bus optimized by dynamic programming", Applied Energy 2017, 185, 1633-1643.
[19] C. Maino, D. Misul, A. Musa, E. Spessa, "Optimal mesh discretization of the dynamic programming for hybrid electric vehicles", Applied Energy 2021, vol. 292, no. 116920.
[20] Sánchez M., Delprat S., Hofman T., "Energy management of hybrid vehicles with state constraints: A penalty and implicit Hamiltonian minimization approach", Applied Energy 2020, vol. 260, no. 114149.
[21] Xie S., Hu X., Xin Z., Brighton J., "Pontryagin's minimum principle based model predictive control of energy management for a plug-in hybrid electric bus", Applied energy 2019, vol. 236, pp. 893-905.
[22] Onori S., Tribioli L., "Adaptive Pontryagin's Minimum Principle supervisory controller design for the plug-in hybrid GM Chevrolet Volt", Applied Energy 2015, vol. 147, pp. 224-234.
[23] Zhang S., Xiong R., Zhang, C., "Pontryagin's minimum principle-based power management of a dual-motor-driven electric bus. Applied energy 2015, vol. 159, pp. 370-380.
[24] C. Hou, M. Ouyang, L. Xu, H. Wang, "Approximate Pontryagin's minimum principle applied to the energy management of plug-in hybrid electric vehicles", Applied Energy 2014; 115: 174-89.
[25] Zhuang,W., Zhang X., Ding Y., Wang, L., Hu, X., "Comparison of multi-mode hybrid powertrains with multiple planetary gears", Applied energy 2016, vol. 178, pp. 624-632.
[26] Zhuang W., Zhang X., Li D., Wang L.,Yin G., "Mode shift map design and integrated energy management control of a multi-mode hybrid electric vehicle", Applied Energy 2017, 204, 476-488.
[27] Qin Z., Luo Y., Zhuang W., Pan Z., Li K.. Peng H., "Simultaneous optimization of topology, control and size for multi-mode hybrid tracked vehicles, Applied energy 2018, vol. 212, pp. 1627-1641.
[28] Anselma P. G., Biswas A., Belingardi G., Emadi A., "Rapid assessment of the fuel economy capability of parallel and series-parallel hybrid electric vehicles", Applied Energy 2020, 275, 115319.
[29] Anselma PG, Huo Y, Roeleveld J, Belingardi G, Emadi A., "Slope-weighted energybased rapid control analysis for hybrid electric vehicles", IEEE Trans Veh Technol 2019;68(5):4458–66.
[30] W. Zhuang, S.L. Eben, X. Zhang, D. Kum, Z. Song, G. Yin, J. Ju, "A survey of powertrain configuration studies on hybrid electric vehicles", Applied Energy 2020; 262: 114553.
[31] Zhang S., Hu X., Xie S., Song Z., Hu L., Hou, C., "Adaptively coordinated optimization of battery aging and energy management in plug-in hybrid electric buses", Applied Energy 2019, 256, 113891.
[32] G. Rizzoni, L. Guzzella, B. M. Baumann, "Unified modeling of hybrid electric vehicle drivetrains," in IEEE/ASME Transactions on Mechatronics, vol. 4, no. 3, pp. 246-257, 1999.
[33] Bloomberg. Gasoline Prices around the World: The Real Cost of Filling Up. Available online: https://www.bloomberg.com/graphics/gas-prices/#20202:Italy:EUR:l (accessed on 28 October 2021).
[34] Eurostat. Electricity Prices for Household Consumers—Bi-Annual Data. Available online: https://ec.europa.eu/eurostat/databrowser/view/nrg_pc_204/default/table?lang=en (accessed on 28 October 2021).

[35] Passmore M., Wheals J., Patel A., "Model for Drivers' Perception of Vehicle Performance," SAE Technical Paper 940386, 1994.
[36] Xu B., Rathod D., Zhang D., Yebi A., Zhang X., Li X., Filipi Z., "Parametric study on reinforcement learning optimized energy management strategy for a hybrid electric vehicle", Applied Energy 2020, vol. 259, 114200.
[37] Biswas A., Anselma P. G., Rathore A., Emadi, A., "Effect of coordinated control on real-time optimal mode selection for multi-mode hybrid electric powertrain", Applied Energy 2021, 289, 116695.
[38] R. Bellman, R. Kalaba, "Dynamic programming and adaptive processes: Mathematical foundation," in IRE Transactions on Automatic Control, vol. AC-5, no. 1, pp. 5-10, 1960.
[39] J. Lempert, B. Vadala, K. Arshad-Aliy, J. Roeleveld, A. Emadi, "Practical Considerations for the Implementation of Dynamic Programming for HEV Powertrains," 2018 IEEE Transportation Electrification Conference and Expo (ITEC), Long Beach, CA, USA, 2018, pp. 755-760.
[40] Bruck L., Lempert A., Amirfarhangi Bonab S., Lempert J., Biswas A. Anselma P.G. et al., "A Dynamic Programming Algorithm for HEV Powertrains Using Battery Power as State Variable," SAE Technical Paper 2020-01-0271, 2020.
[41] O. Sundstrom, L. Guzzella, "A generic dynamic programming Matlab function," 2009 IEEE Control Applications, (CCA) & Intelligent Control, (ISIC), St. Petersburg, Russia, 2009, pp. 1625-1630.
[42] Miretti F., Misul D. and Spessa E., "DynaProg: Deterministic Dynamic Programming solver for finite horizon multi-stage decision problems", *SoftwareX*, 14, 100690, 2021.
[43] Zhang, S., Xiong, R., "Adaptive energy management of a plug-in hybrid electric vehicle based on driving pattern recognition and dynamic programming", Applied Energy, 155, 68-78, 2015.
[44] Cipek M., Kasać J., Pavković D., Zorc D., "A novel cascade approach to control variables optimisation for advanced series-parallel hybrid electric vehicle power-train", Applied Energy, 276, 115488, 2020
[45] P. Elbert, S. Ebbesen, L. Guzzella, "Implementation of Dynamic Programming for $n$-Dimensional Optimal Control Problems With Final State Constraints," in IEEE Transactions on Control Systems Technology, vol. 21, no. 3, pp. 924-931, May 2013.
[46] Zhuan X., Xia X., "Optimal operation scheduling of a pumping station with multiple pumps", Applied Energy 2013, vol. 104, pp. 250-257.
[47] N. Kim, S. Cha, H. Peng, "Optimal Control of Hybrid Electric Vehicles Based on Pontryagin's Minimum Principle", IEEE Transactions on Control Systems Technology, vol. 19, no. 5, pp. 1279-1287, 2011.
[48] United States Environmental Protection Agency, "Compliance and Fuel Economy Data - Annual Certification Data for Vehicles, Engines, and Equipment", [online] https://www.epa.gov/compliance-and-fuel-economy-data/annual-certification-data-vehicles-engines-and-equipment (accessed 15 Jun 2021).
[49] G. Alix, J. Dabadie, G. Font, "An ICE Map Generation Tool Applied to the Evaluation of the Impact of Downsizing on Hybrid Vehicle Consumption", SAE Technical Paper 2015-24-2385, 2015.
[50] F. Le Berr, A. Abdelli, D.-M. Postariu, R. Benlamine, "Design and Optimization of Future Hybrid and Electric Propulsion Systems: An Advanced Tool Integrated in a Complete Workflow to Study Electric Devices", Oil & Gas Science and Technology, vol. 67, no. 4, pp. 547-562, 2012.
[51] Anselma P. G., Kollmeyer P., Lempert J., Zhao Z., Belingardi G., Emadi A., "Battery state-of-health sensitive energy management of hybrid electric vehicles: Lifetime prediction and ageing experimental validation", Applied Energy 2021, vol. 285, no. 116440.
[52] Vora A.P., Jin X., Hoshing V., Saha T., Shaver G., Varigonda, S. et al., "Design-space exploration of series plug-in hybrid electric vehicles for medium-duty truck applications in a total cost-of-ownership framework", Applied energy 2017, vol. 202, pp. 662-672.
[53] Finesso R., Spessa E., Venditti, M., "Cost-optimized design of a dual-mode diesel parallel hybrid electric vehicle for several driving missions and market scenarios. Applied energy 2016, vol. 177, pp. 366-383.
[54] Hegde B., Ahmed Q., Rizzoni, G., "Velocity and energy trajectory prediction of electrified powertrain for look ahead control", Applied Energy 2020, vol. 279, no. 115903.
[55] Xie S., Qi S., Lang K., Tang X., Lin X., "Coordinated management of connected plug-in hybrid electric buses for energy saving, inter-vehicle safety, and battery health", Applied Energy 2020, vol. 268, no. 115028.